Molecular Motions and Phase Transitions in Solid $CH_3NH_3PbX_3$ (X = Cl, Br, I) as Studied by NMR and NQR *

Qiang Xu, Taro Eguchi, Hirokazu Nakayama, Nobuo Nakamura **
and Michihiko Kishita

Institute of Chemistry, College of General Education and
** Department of Chemistry, Faculty of Science, Osaka University, Toyonaka, Osaka 560, Japan

Z. Naturforsch. **46 a**, 240–246 (1991); received November 9, 1990

The temperature dependence of ^{35}Cl, ^{81}Br, and ^{127}I NQR frequencies and ^1H spin-lattice relaxation times (T_1) for $CH_3NH_3PbX_3$ (X = Cl, Br, I) was measured through the successive phase transitions in these solids. The isotropic reorientation of the $CH_3NH_3^+$ ions takes place in the higher-temperature phases (tetragonal [I4/mcm] and cubic) of the three salts ($E_a = 11$ kJ mol^{-1}). T_1's in the lowest-temperature phases (orthorhombic) indicate that the cations undergo correlated C_3-reorientation in the chloride ($E_a = 5.45$ kJ mol^{-1}) and in the iodide ($E_a = 5.80$ kJ mol^{-1}), whereas correlated ($E_a = 2.40$ kJ mol^{-1}) and uncorrelated ($E_a = 7.50$ kJ mol^{-1}) C_3-reorientations are excited in the bromide. It is also revealed that the rotational tunneling of the cations governs T_1 at low-temperature region in the orthorhombic phases of these salts.

Key words: NMR, NQR, Methylammonium lead(II) halides, Molecular motion, Rotational tunneling.

Introduction

Methylammonium lead(II) halides, $CH_3NH_3PbX_3$ (X = Cl, Br, I) assume the perovskite-type structure (cubic) in the highest-temperature phases [1, 2]. The crystals consist of corner-shared $[PbX_6]^{4-}$ octahedra and the $CH_3NH_3^+$ ions located inside the cuboctahedral cages formed by these octahedra. Isotropic reorientation of the cations occurs in the cubic phases [2–4].

On lowering the temperature, these substances undergo successive phase transitions [2, 3]. For the chloride, the cubic phase (Pm3m) transforms to a tetragonal phase (P4/mmm) at 178.8 K, and to an orthorhombic phase ($P222_1$) at 172.9 K. For the bromide, the cubic phase (Pm3m) transforms to a tetragonal phase (I4/mcm) at 236.9 K, to another tetragonal phase (P4/mmm) at 155.1 K, and to an orthorhombic phase ($Pna2_1$) at 149.5 K. For the iodide, the cubic phase (Pm3m) transforms to a tetragonal phase (I4/mcm) at 327.4 K, and to an orthorhombic phase ($Pna2_1$) at 162.2 K. All these transitions are of the first order [3, 5]. In the I4/mcm phases of the bromide and the iodide, the $CH_3NH_3^+$ ions undergo isotropic reorientation, while in the lower-temperature phases the reorientation of C–N axes seems to be frozen [3].

Although the motion of $CH_3NH_3^+$ in the cubic phase has been examined to some extent, few studies have been reported on the motions of $CH_3NH_3^+$ in the intermediate- and the lowest-temperature phases. Furthermore, the nature and mechanisms of the successive phase transitions have not yet been studied. In order to shed light on these points, we measured ^1H spin-lattice relaxation times over a wide range of temperature in $CH_3NH_3PbX_3$ (X = Cl, Br, I). The frequencies of ^{35}Cl, ^{81}Br and ^{127}I NQR (nuclear quadrupole resonance) were also measured to derive information on the crystal symmetry and a possible relation between the cationic motion and the successive phase transitions.

The following nomenclature will be used to represent the phases of the salts: phase I for cubic phase; phase II for tetragonal phase (I4/mcm); phase II* for tetragonal phase (P4/mmm); phase III for orthorhombic phase.

Experimental

Methylammonium lead(II) halides were prepared by the method described in [2]. Samples were then recrystallized by cooling the concentrated aqueous solution

* A part of the results was presented at the Xth International Symposium on Nuclear Quadrupole Resonance Spectroscopy, Takayama, Japan, August 22–26, 1989.

Reprint requests to Dr. Eguchi, Institute of Chemistry, College of General Education, Osaka University, Toyonaka, Osaka 560, Japan.

0932-0784 / 91 / 0300-0240 $ 01.30/0. – Please order a reprint rather than making your own copy.

of the respective HX (X = Cl, Br, I) acid from 100 °C to room temperature. In the case of $CH_3NH_3PbCl_3$ an excess of $CH_3NH_3^+$ (ca. 8 mol per 1 mol $CH_3NH_3PbCl_3$) was added to the solution to prevent co-precipitation of $PbCl_2$. For $CH_3NH_3PbI_3$ the temperature was kept above 50 °C in order to avoid the formation of hydrate crystals [2, 3]. All the salts thus prepared were dried under vacuum at 90 °C for 3 days. The purity of the salts was found to be higher than 99% by elemental analyses. All the transition temperatures determined by DTA were in good agreement with those reported previously [2, 3]. Specimens used for the NMR and NQR measurements were sealed in glass tubes (12 mm $\varnothing \times 30$ mm) with a small amount of helium gas.

Proton spin-lattice relaxation times, T_1, were measured at the Larmor frequencies of 40.4, 20.4 and 10.4 MHz with a MATEC pulsed spectrometer (Model 5100 system) and a JEOL pulsed spectrometer (JNM-FSE-60SS) with $\pi/2-\tau-\pi/2$ pulse sequence. The experimental uncertainties were estimated to be within $\pm 5\%$ except for the T_1 of the bromide below 30 K, where the error in T_1 increased up to $\pm 10\%$ due to the difficulty in controling the temperature.

The NQR frequencies for ^{35}Cl in the chloride and for ^{81}Br in the bromide were determined by Fourier transform (FT) of the free induction decays (FID) measured with the MATEC pulsed spectrometer. The experimental errors were estimated to be within ± 0.5 kHz. For the ^{127}I NQR measurements a super-regenerative spectrometer was used. The uncertainty in the frequency was within ± 3 kHz.

Results

NQR Spectra

The cubic phases of $CH_3NH_3PbCl_3$ and $CH_3NH_3PbBr_3$ give single (^{35}Cl or ^{81}Br) NQR lines as listed in Table 1. This is consistent with the crystal structure data [2, 3]. The ^{35}Cl NQR signal in the chloride disappeared below the phase transition point (T_{I-II^*}) as shown in Fig. 1, the reason of which is unclear. A very small but positive temperature-coefficient of the resonance frequency was observed in the cubic phase as having often been observed in complex compounds [6].

In the case of the bromide, the single ^{81}Br NQR line in phase I splits into two lines with a very small jump at T_{I-II} as shown in Figure 2. The discontinuity of

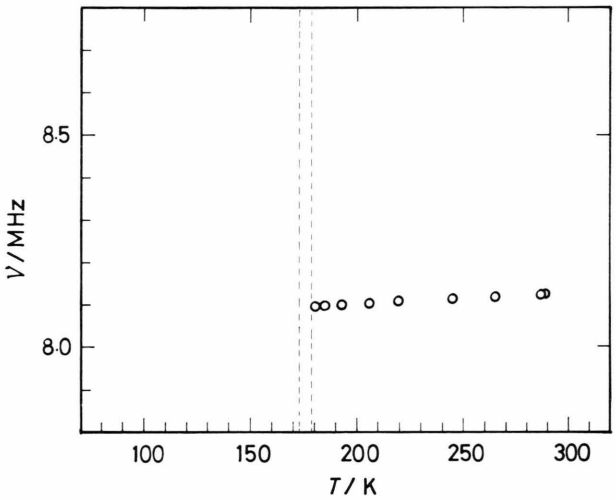

Fig. 1. Temperature dependence of ^{35}Cl NQR frequency in solid $CH_3NH_3PbCl_3$.

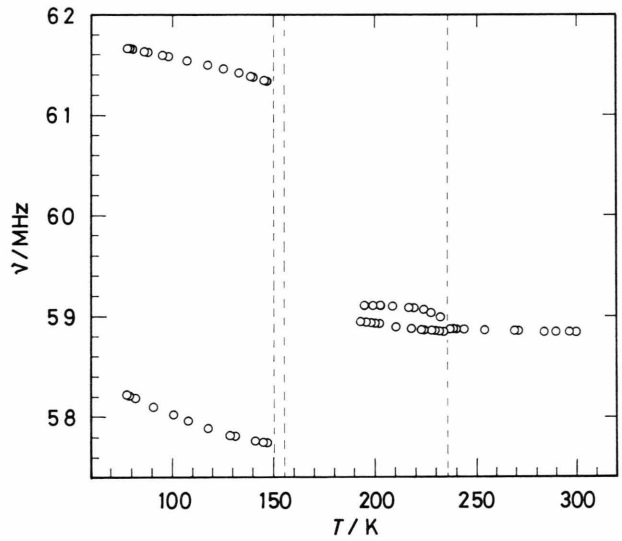

Fig. 2. Temperature dependence of ^{81}Br NQR frequencies in solid $CH_3NH_3PbBr_3$.

NQR frequencies at the transition point suggests that this transition is of the first-order but, strictly speaking, involves a character of the second-order. This result is in accordance with the thermodynamic studies [3, 5]. The small difference in frequency between the two resonance lines strongly suggests that the transition is mainly associated with a slight tetragonal distortion of the anion lattice, and is almost unaffected by the motion of the cations. This is also supported by the ^1H NMR results discussed in the next section.

Table 1. NQR parameters in solid $CH_3NH_3PbX_3$ (X = Cl, Br, I).

Compound	Nucleus		T/K	ν/MHz	(e^2Qq/h)/MHz	η
$CH_3NH_3PbCl_3$	^{35}Cl		298	8.128		
$CH_3NH_3PbBr_3$	^{79}Br		298	70.451		
			77.4	69.701, 73.819		
	^{81}Br		298	58.842		
			77.4	58.239, 61.678		
$CH_3NH_3PbI_3$	^{127}I	Site A	289	83.430, 166.840	556.139	0.010
			77.4	85.973, 160.192	539.974	0.241
		Site B	289	82.062, 164.094	573.063	0.012
			77.4	84.895, 159.161	536.132	0.229

The signals of these two lines become weak on lowering the temperature. No signal could be detected between 180.0 and 150.5 K. Two lines appear again in phase III, as shown in Figure 2. The lower-frequency line is twice as intense as the higher one. This fact shows the presence of only two kinds of inequivalent Br atoms in a unit cell. The separation of these lines is about 15 times as large as that in phase II.

In the iodide ^{127}I NQR frequencies were determined at 77.4 and 289 K. Two pairs of resonance lines were observed at each temperature, corresponding to the transitions $(\pm 1/2 \leftrightarrow \pm 3/2)$ and $(\pm 3/2 \leftrightarrow \pm 5/2)$, respectively. In Table 1, the assignment of the resonance frequencies, the nuclear quadrupole coupling constant, e^2Qq/h, and the asymmetry parameter, η, are listed.

The four resonance lines at 289 K indicate the existence of two inequivalent iodine sites in a unit cell, which is consistent with the tetragonal structure. It is worth noting that the difference in the electric field gradients (efg) at these two sites is large in comparison with that in phase II (tetragonal) of the bromide. This suggests that a large tetragonal distortion of the anion lattice occurs in the iodide. The only four NQR lines observed at 77.4 K suggest that there are two inequivalent iodine sites even in the orthorhombic phase (III). It also follows that the asymmetry parameters of the efg's for both sites are considerably large in phase III of the iodide.

Proton Spin-Lattice Relaxation Times

1. $CH_3NH_3PbCl_3$

Figure 3 shows the proton spin-lattice relaxation times (T_1) at 10.4, 20.4, and 40.4 MHz in the chloride. In phase III a $\log T_1$ vs. $1/T$ curve exhibits a single deep T_1 minimum (22 ms at 20 MHz), the value of which depends linearly on the Larmor frequency.

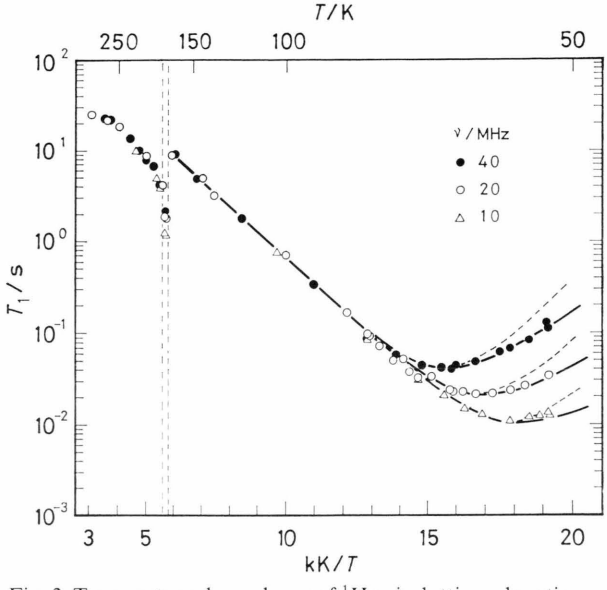

Fig. 3. Temperature dependence of ^1H spin-lattice relaxation times in solid $CH_3NH_3PbCl_3$. The broken lines represent the theoretical curves according to the BPP formula. The solid lines are the calculated T_1 curves by taking account of the rotational tunneling and the correlated C_3-reorientation, (2). The parameters used in the calculation are shown in Table 2.

The magnetization recovery after the second $\pi/2$ pulse was nonexponential in the vicinity of the minimum. This nonexponential behavior may mainly be attributed to the cross correlation of dipolar interactions in a CH_3 or NH_3 group [7, 8]. Use was made of the initial slope of the semilog plot of the magnetization recovery vs. time to determine T_1 [9].

The abrupt change of T_1 indicates that the transition III – II* is of the first order [3, 5]. In addition, FID

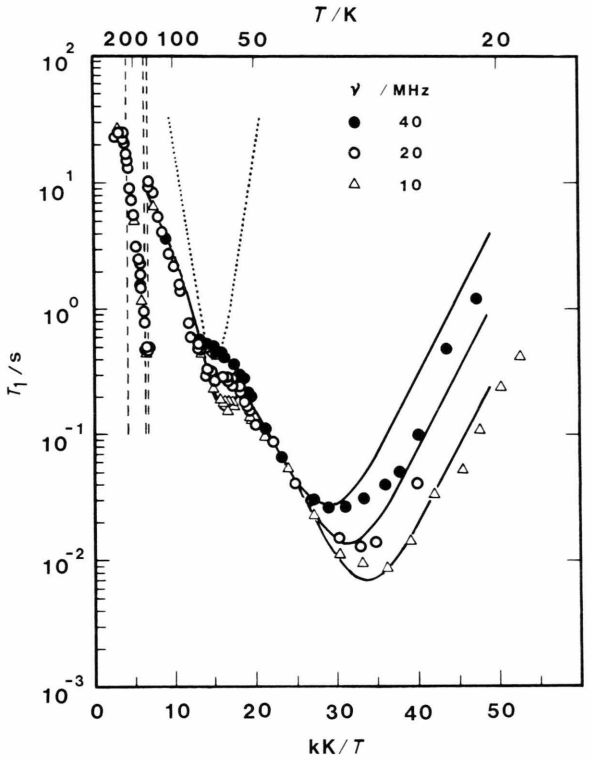

Fig. 4. Temperature dependence of ^1H spin-lattice relaxation times in solid $CH_3NH_3PbBr_3$. The solid lines are the calculated T_1 curves by considering the two modes of the cation motion; the correlated reorientation and the uncorrelated reorientation (internal rotation) of $CH_3NH_3^+$, (3). The dotted curve represents the contribution of the uncorrelated reorientation at 20 MHz. The parameters used are shown in Table 2.

signals become longer above this transition temperature. In phase II*, the temperature dependence of T_1 could not be measured because this phase exists only over a narrow temperature range (ca. 6 K). However, a peculiar frequency dependence of T_1 was observed: T_1 at 10 MHz is ca. 1.2 s, while the T_1's at 20 and 40 MHz have almost the same values of ca. 2 s.

The II*–I phase transition is accompanied by a slight discontinuous change in T_1. This reflects the first-order nature of this transition [3]. Above the transition temperature, FID signals become longer again. T_1 is independent of the Larmor frequency and increases monotonously on heating in phase I.

2. $CH_3NH_3PbBr_3$

In phase III, a deep T_1 minimum, e.g., 16 ms at 20 MHz, appears at ca. 32 K, a temperature which is lower than that in the chloride (Figure 4). A shallow dip was recognized at ca. 67 K. The T_1 value of the dip is about 20 times as large as that of the minimum. The magnetization recovery was nonexponential in the temperature range between the minimum and the dip. The slope of the log T_1 vs. T^{-1} plot on the high-temperature side of the dip is significantly larger than that on the low-temperature side of the dip.

At T_{III-II^*}, T_1 drops suddenly from 10 s to 0.45 s due to the first-order nature of this transition [3, 5]. The temperature range of phase II* is too narrow to determine the temperature dependence of T_1. However, it

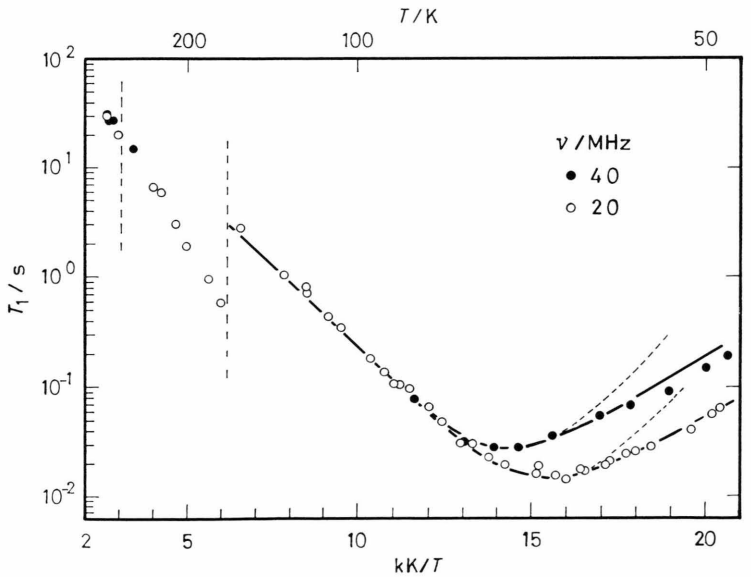

Fig. 5. Temperature dependence of ^1H spin-lattice relaxation times in solid $CH_3NH_3PbI_3$. The broken lines are the theoretical curves according to the BPP formula. The solid lines are the calculated T_1 curves for which the tunneling motion is taken into account. See also Table 2.

was confirmed that T_1 has no frequency dependence within the experimental error.

The T_1 curve seems to change continuously at T_{II^*-II}. In phase II, T_1 increases monotonously with increasing temperature. T_1 again varies continuously at T_{II-I}.

3. $CH_3NH_3PbI_3$

As shown in Fig. 5, a single T_1 minimum (15 ms at 20 MHz) was observed (at ca. 65 K) in phase III. A discontinuous change of T_1 occurs at the III–II transition point, indicating that the transition is of the first-order. T_1 increases monotonously with increasing temperature in phase II, and continues almost smoothly through T_{II-I}.

Discussion

We will next give quantitative analyses of the spin-lattice relaxation data in relation to specific molecular motions in the individual phases.

1. Phases I (cubic) and Phases II (tetragonal, I4/mcm)

In each cubic phase of the salts, the isotropic reorientation of the $CH_3NH_3^+$ ions has been confirmed by ^2H NMR [3] and ^1H second-moment measurements [4].

T_1 varies continuously, and no discernible change in FID was observed through the I–II transition of the bromide and the iodide. Hence, the phase transition gives no significant effect on the motional state of the $CH_3NH_3^+$ ions, as expected from the NQR experiments in the previous section, and the overall (isotropic) reorientation of the $CH_3NH_3^+$ ions is highly excited in phases II.

According to the ^2H NMR studies [3], in phase II, the activation energies (E_a) for the isotropic reorientation of the cations vary from 13.80 to 9.05 kJ mol^{-1} in the bromide, and from 13.13 to 6.54 kJ mol^{-1} in the iodide, with increasing temperature. In conflict with these results, our present work shows linear $\log T_1$ vs. $1/T$ plots for both salts – the activation energies of the isotropic reorientation are independent of temperature. The slopes gave activation energies of 11.9 and 10.4 kJ mol^{-1} for the bromide and the iodide, respectively (Table 2). This is also supported by the fact that the ^{81}Br NQR frequencies have almost no temperature dependence.

A T_1 maximum observed in each cubic phase of $CH_3NH_3PbCl_3$ and $CH_3NH_3PbBr_3$ shows no frequency dependence, suggesting that a relaxation process other than the magnetic dipolar relaxation contributes to the ^1H T_1 observed. The most feasible relaxation mechanism is the spin-rotation within the $CH_3NH_3^+$ ions [10].

2. Phases II (tetragonal, P4/mmm)*

Both $CH_3NH_3PbCl_3$ and $CH_3NH_3PbBr_3$ are tetragonal (P4/mmm) over a narrow temperature range.

The time constants of FID's ($\propto T_2^*$) are twice those in phases III. This is probably due to a sort of small-angle precession of $CH_3NH_3^+$ [4].

The significantly short T_1 value at 10 MHz in the chloride may be caused by the effect of cross-relax-

Table 2. Activation energies (E_a) and inverse frequency factors (τ_0) of molecular motions in solid $CH_3NH_3PbX_3$ (X = Cl, Br, I).

Compound	Phase	E_a/kJ mol^{-1}	$\tau_0/10^{-13}$ s	Motional mode
$CH_3NH_3PbCl_3$	Pm3m	10.5 ± 0.7	–	Isotropic reorientation
	P4/mmm	–	–	–
	$P222_1$	5.45	1.0	Correlated C_3 reorientation
		(2.2	2.0×10^3)	Tunneling rotation
$CH_3NH_3PbBr_3$	Pm3m, I4/mcm	11.9	–	Isotropic reorientation
	P4/mmm	–	–	–
	$Pna2_1$	7.50	5.7×10^{-2}	Uncorrelated C_3 reorientation
		2.40	5.9	Correlated C_3 reorientation
$CH_3NH_3PbI_3$	Pm3m, I4/mcm	10.4	–	Isotropic reorientation
	$Pna2_1$	5.80	1.25	Correlated C_3 reorientation
		(2.2	2.0×10^3)	Tunneling rotation

The values in parentheses are estimated for the tunneling mode: the energy between the ground and the first excited torsional state E_{01}, and the pre-exponential factor τ_0' in (2).

ation between ^{35}Cl and ^1H, because there is a possibility that the ^{35}Cl NQR signal at about 8 MHz (Fig. 1) overlaps with the proton signal.

3. Phases III (orthorhombic)

The lowest-temperature phases of all salts studied here are orthorhombic [2]. In these orthorhombic phases, the orientation of the $CH_3NH_3^+$ ions is ordered with respect to the direction of the C–N axes [3, 4], while the CH_3- and NH_3-groups can rotate about the C_3-symmetry axis (C–N axis) of each cation.

Two kinds of models have been taken into account to describe such uniaxial reorientation of the $CH_3NH_3^+$ ions. One is the in-phase reorientation of the CH_3- and NH_3-groups (referred to as correlated reorientation), and the other is the independent reorientation of the CH_3- and NH_3-groups from each other (referred to as uncorrelated reorientation) [11, 12].

A single minimum of T_1 was observed in $CH_3NH_3PbCl_3$ and $CH_3NH_3PbI_3$. These minima are obviously due to the C_3-reorientation of $CH_3NH_3^+$. The activation energies estimated from the slopes of the high-temperature sides of the T_1 minima are 5.45 kJ mol^{-1} for the chloride and 5.80 kJ mol^{-1} for the iodide. Since these values are much smaller than 8 kJ mol^{-1}, the height of the barrier for the internal rotation of $CH_3NH_3^+$ [11, 12], the motion responsible for the relaxation can be assigned to the correlated C_3-reorientation of the cations. The absolute values of these minima, however, cannot be interpreted by the well-known BPP theory assuming the thermally activated reorientation of $CH_3NH_3^+$ and assuming the normal geometry of the cation. The experimental values of the minima are about twice the theoretical ones, and the experimental $\log T_1$ vs. $1/T$ plots are not symmetric, contrary to the prediction of the BPP theory. These discrepancies between the experimental and the theoretical T_1's can be ascribed to the influence of the tunneling rotation of the CH_3- and NH_3-groups on the dipolar relaxation in the lowest-temperature phase [13–18].

In the presence of the tunneling rotation, the correlation time τ_c corresponds to the life time of the tunneling level [13–18]. In the low-temperature limit τ_c is therefore approximated by

$$\tau_c = \tau_0' \exp(E_{01}/RT), \tag{1}$$

where E_{01} is the energy difference between the two lowest torsional states. At intermediate temperatures, the contribution from the higher torsional states becomes progressively important, and at high temperatures, the stochastic activation over the barrier becomes dominant. In the first approximation, however, we take account of (1) and the thermal processes to represent the actual correlation time over the whole temperature region [16, 18] as

$$\tau_c^{-1} = \tau_0'^{-1} \exp(-E_{01}/RT) + \tau_0^{-1} \exp(-E_a/RT). \tag{2}$$

The results of fitting are shown by the solid curves in Figs. 3 and 5, for $CH_3NH_3PbCl_3$ and for $CH_3NH_3PbI_3$, respectively. It is clear that the calculated curves agree well with the experimental data. The parameters used for the fitting are listed in Table 2.

In the case of phase III of $CH_3NH_3PbBr_3$, a deep T_1 minimum appears with a shallow dip on its high-temperature side. T_1 near the shallow dip depends on the Larmor frequency, so that another dipolar-relaxation process starts to contribute in this temperature region. Since the dip is very shallow and the slope above it is slightly larger than that below it, the motion responsible for the relaxation is unambiguously assigned to the uncorrelated C_3-reorientation of $CH_3NH_3^+$. In the presence of both correlated and uncorrelated reorientations, the spin-lattice relaxation rate for a single $CH_3NH_3^+$ ion is written as [11, 19]

$$T_1^{-1} = \sum_i K_i \{\tau_{ci}/(1+\omega_0^2 \tau_{ci}^2) + 4\tau_{ci}/(1+4\omega_0^2 \tau_{ci}^2)\}, \tag{3}$$

and

$$\tau_{ci} = \tau_{0i} \exp(E_{ai}/RT), \tag{4}$$

where $i = 1, 2$, and $\tau_{c1} \ll \tau_{c2}$ is assumed. The first term of (3) is due to the contribution from the correlated C_3-reorientation with the correlation time τ_{c1}, and the second due to the contribution from the uncorrelated reorientation with the relative correlation time τ_{c2} of the CH_3- and NH_3-groups [11].

Using the coupling constants of $K_1 = 5.9 \times 10^{-13}$ and $K_2 = 5.7 \times 10^{-15}\ s^{-2}$, we simulated the experimental relaxation data with (3) and obtained the values of E_a and τ_0 for the two modes as listed in Table 2. The calculated T_1's are shown by the solid lines in Figure 4. It is obvious that the calculated T_1's near the dip agree excellently with the experiments. The uncorrelated reorientation of $CH_3NH_3^+$, therefore, contributes to the relaxation behavior above 50 K in the orthorhombic phase of the bromide. The calculated value of the T_1 minimum due to this mode is 440 ms at 20 MHz, which is comparable with the theoretical

value (460 ms) reported previously for the uncorrelated reorientation [11]. The values of E_a, 7.50 kJ mol^{-1}, can be compared with the heights of internal-rotation barriers, 8.5 kJ mol^{-1} in $(CH_3NH_3)_2PtCl_6$, and 7.2 kJ mol^{-1} in $(CH_3NH_3)_2SnCl_6$ [11].

Below 50 K the correlated reorientation of $CH_3NH_3^+$ becomes the dominant relaxation mechanism and has an activation energy of $E_a = 2.40$ kJ mol^{-1} in the bromide. It is to be noted that this value is much smaller (almost 1/2) than those in the other two salts (see Table 2).

The E_a values of the uniaxial-reorientation barriers for the $CH_3NH_3^+$ ion decrease in the order Cl > Br > I in the series of CH_3NH_3X [9, 20, 21] and of $(CH_3NH_3)_2TeX_6$ [12] (X = Cl, Br, I). This is probably related to the strength of N–H $\cdots$ X type hydrogen bonds. In the present case, however, the E_a values of the correlated C_3-reorientation in $CH_3NH_3PbX_3$ are out of the order. A possible interpretation for this is that the difference in the volume of the cavities formed by the X atoms in these PbX_3 complexes is dominantly related to the rotational barrier for $CH_3NH_3^+$. Using the lattice parameters determined by Poglitsch [2] and the ionic radii of Pb^{2+} and X^-, we estimated the volumes of the X_{12} cages. It showed that the contraction of the X_{12} cages due to transformation from the cubic to the orthorhombic phase is largest in the iodide among these three salts. This fact suggests that in phase III the contraction of the I_{12} cage gives rise to the high potential barrier. On the other hand, the rate of the contraction of the Br_{12} and the Cl_{12} cages is almost the same. Therefore, the rotational barrier can be lower in the bromide than in the chloride if we take into account that the N–H $\cdots$ X hydrogen bonds are stronger in the chloride than in the bromide.

The experimental T_1 data in the orthorhombic phase of the bromide can be interpreted qualitatively by the discussion described above, but there still exists a discrepancy between the observed and the calculated T_1's below the T_1 minimum. The experimental value of the T_1 minimum is larger than the theoretical one, and the observed T_1 curve near the minimum exhibits asymmetric behavior. We have already seen a similar feature in the chloride and the iodide and have interpreted it by introducing a model of tunneling-assisted relaxation. This mechanism may also work in the bromide at low temperatures. However, since the apparent activation energy of the correlated C_3-reorientation is remarkably low in the bromide, it is hardly possible to distinguish the stochastic reorientation from the possible tunneling rotation. We are planning to clarify this point by performing experiments on partially deuterated derivatives.

To summarize: In phases III (orthorhombic), the rotational tunneling of $CH_3NH_3^+$ about the C–N axis contributes to the ^1H spin-lattice relaxation in the lowest-temperature region, and the thermally activated correlated C_3-reorientation becomes to govern the relaxation on heating. In the case of the bromide the uncorrelated reorientation is responsible for the relaxation in the high-temperature region of phase III. The cations undergo a small-angle precession in phases II* (tetragonal, P4/mmm). Overall reorientation occurs in phases II (tetragonal, I4/mcm) as well as in phases I (cubic).

[1] D. Weber, Z. Naturforsch. **33b,** 1443 (1978).
[2] A. Poglitsch and D. Weber, J. Chem. Phys. **87,** 6373 (1987).
[3] O. Knop, R. E. Wasylishen, M. A. White, T. S. Cameron, and M. J. M. V. Oort, Can. J. Chem. **68,** 412 (1990).
[4] Y. Furukawa and D. Nakamura, private communication.
[5] N. Onoda, T. Matsuo, and H. Suga, private communication.
[6] D. Nakamura, R. Ikeda, and M. Kubo, Coord. Chem. Rev. **17,** 281 (1975).
[7] R. L. Hilt and P. S. Hubbard, Phys. Rev. A **134,** 392 (1964).
[8] S. Emid, R. J. Baarda, J. Smidt, and R. A. Wind, Physica B+C (Amsterdam) **93,** 327 (1978).
[9] S. Albert and J. A. Ripmeester, J. Chem. Phys. **58,** 541 (1973).
[10] R. Ikeda and C. A. McDowell, Chem. Phys. Lett. **14,** 389 (1972).
[11] R. Ikeda, Y. Kume, D. Nakamura, Y. Furukawa, and H. Kiriyama, J. Magn. Reson. **24,** 9 (1976).
[12] Y. Furukawa, H. Kiriyama, and R. Ikeda, Bull. Chem. Soc. Japan **54,** 103 (1981).
[13] J. Haupt, Z. Naturforsch. **26a,** 1578 (1971).
[14] W. Müller-Warmuth, R. Schuler, M. Prager, and A. Kollmar, J. Chem. Phys. **69,** 2382 (1978).
[15] S. Takeda and H. Chihara, J. Magn. Reson. **54,** 285 (1983).
[16] S. Takeda and H. Chihara, J. Magn. Reson. **56,** 48 (1984).
[17] D. J. Ligthelm, R. A. Wind, and J. Smidt, Physica B **100,** 175 (1980).
[18] T. Eguchi and H. Chihara, J. Magn. Reson. **76,** 143 (1988).
[19] D. E. Woessner, J. Chem. Phys. **42,** 1855 (1965).
[20] H. Ishida, R. Ikeda, and D. Nakamura, J. Phys. Chem. **82,** 1003 (1982).
[21] H. Ishida,. R. Ikeda, and D. Nakamura, Bull. Chem. Soc. Japan **59,** 915 (1986).